An *ab initio* study of electronic and structural properties of Mn in a GaAs environment

2009 J. Phys.: Condens. Matter 21 485504

(http://iopscience.iop.org/0953-8984/21/48/485504)

J. Phys.: Condens. Matter **21** (2009) 485504 (10pp) doi:10.1088/0953-8984/21/48/485504

An *ab initio* study of electronic and structural properties of Mn in a GaAs environment

A Z AlZahrani[1], G P Srivastava[1], R Garg[2] and M A Migliorato[2]

[1] School of Physics, University of Exeter, Stocker Road, Exeter EX4 4QL, UK
[2] School of Electrical and Electronic Engineering, University of Manchester, Sackville Street, Manchester M60 1QD, UK

Received 22 September 2009, in final form 19 October 2009
Published 11 November 2009
Online at stacks.iop.org/JPhysCM/21/485504

Abstract

Based on *ab initio* calculations, we have investigated the atomic geometry, electronic properties and magnetic properties of Mn incorporation in GaAs. The inclusion of the Hubbard potential U in the calculation (namely with the σGGA + U scheme) results in the optimized geometry being contracted by approximately 2% relative to the relaxed geometry obtained by the (σGGA) method. Within both the σGGA and σGGA + U schemes the Mn impurity in bulk GaAs behaves like a d-hole with the majority spin state lying at 0.25 eV above the Fermi level. Theoretically simulated STM images for Mn/GaAs(110) indicate round protrusions at As sites and Ga sites, the latter being dependent on the Mn adsorption site (i.e. in different atomic layers). These results are supportive of a previous experimental STM image obtained with a very low Mn concentration.

(Some figures in this article are in colour only in the electronic version)

1. Introduction

Semiconductors containing small amounts of substitutional dopants that provide local magnetic moments are referred to as dilute magnetic semiconductors (DMS). Such materials have the potential to offer an interesting combination of electrical, optical and magnetic properties [1, 2]. In particular, the combination of semiconducting and ferromagnetic properties enables the use of the spin degree of freedom, making DMSs suitable for technological applications in spintronics [3].

(III, Mn)V systems have attracted a great deal of attention and provided a valuable testing ground for DMS properties [2]. Among these, (Ga, Mn)As has gained much more interest due to its relatively high Curie temperature (about 150 K) and compatibility with the well-characterized GaAs environment [1, 4]. It has been reported that the substitution of the Mn atom for the Ga site in GaAs results in a local spin $\frac{5}{2}$ magnetic moment and gives rise to an acceptor state at about 113 meV above the valence band [5]. The ground-state electronic structure of the Mn atom has the [Ar]$3d^5 4s^2$ configuration. Therefore, when Mn substitutes the Ga atom, only three electrons will be needed for completing the bonds with the nearest As atoms. However, two possible configurations are expected to occur for the whole system: either $3d^4$ or $3d^5$ + hole. Several workers, for example [6, 7], have argued these issues but to the best of our knowledge no clear conclusion has been drawn.

The structural and electronic configurations of Mn impurity in the bulk GaAs have been experimentally investigated using cross-sectional scanning tunnelling microscopy (XSTM) [8–11] and scanning tunnelling microscopy (STM) [12–14]. In their works, Yakunin *et al* [12, 14] have demonstrated that the Mn acceptor in (Ga, Mn)As has a highly anisotropic spatial structure due to the presence of a d-wave envelope function in its ground state. They have also observed that the properties of the valence band of the GaAs host take the responsibility for the anisotropy of the Mn acceptor states. This was found to be in agreement with their tight-binding model. Recently, Kitchen *et al* [13] have measured the energy splitting of the Mn acceptor states in GaAs by forming Mn pairs using an atom-by-atom substitution technique. They concluded that the Mn–Mn interaction decays rapidly and becomes anisotropic with the increase of separation between the Mn acceptors. With increased coverage, Jin *et al* [15] have identified a two-dimensional growth of Mn atoms, with magnetic ordering, on GaAs(001).

From the theoretical point of view, the magnetic and electronic properties of the (Ga, Mn)As DMS have been studied in the framework of the local density approximation scheme [7, 16, 17]. In their study, Park *et al* [17] have summarized that the introduction of a Coulomb correlation effect (U) plays an important role in providing a better description of the electronic structure of this DMS. Sandratskii *et al* [16] have reported that the consideration of U in LSDA calculations increases the delocalization of holes and decreases the p–d interaction. Schulthess *et al* [7] have also demonstrated that using standard band structure tools (for example, LSDA) is not enough to describe the electronic structure of DMS. They reported that the use of correction (such as self-interaction correction—SIC) with the exchange–correlation will modify the electronic and magnetic properties of such materials. However, existing works still do not clarify whether a better description of the DMS is provided within the LSDA or LSDA + U. From the surface science point of view, using a cluster model and the extended Hückel theory, Fu *et al* [18] studied the chemisorption properties of Mn atoms on the GaAs(110) surface. Yang *et al* [19] have studied the chemisorption of a single Mn atom on the GaAs(001) surface and found that the preferential adsorption sites are different for the Mn adatom on the Ga face and on the As face. They reported that the Mn atom prefers to be adsorbed at the fourfold hollow site on the Ga face and at the bridge site on the As face. They also found, as expected, that the Mn–As bond is much stronger than that of the Mn–Ga bond.

Despite much available experimental data, a theoretical understanding of the electronic and magnetic properties of the III–V DMS has not yet been fully and unanimously established. In the present work, we perform first-principles calculations to report on the structural, electronic and magnetic properties of the (Ga, Mn)As and Mn/GaAs(110) structures. Details of the equilibrium geometry are described within the generalized gradient approximation of the density functional theory. The magnetic properties of the systems are determined in terms of the magnetic moment, and the electronic properties have been investigated by examining the electronic band structure and simulated STM.

2. Computational method

We carried out these calculations within the density functional theory [20] using the spin-polarized version of a generalized gradient approximation (DFT–σGGA). The Perdew–Burke–Ernzerhof exchange–correlation scheme [21] was considered to treat electron–electron interactions. Electron–ion interactions were treated by using the ultrasoft pseudopotentials [22]. Single-particle Kohn–Sham [23] wavefunctions were expanded in the framework of a plane wave basis set. Test calculations have shown that a kinetic energy cutoff for the wavefunctions equal to 25 Ryd (340 eV) is sufficient to obtain well-converged results for both bulk and surface investigations. Self-consistent solutions of the Kohn–Sham equations were obtained by employing $4 \times 4 \times 4$ and $3 \times 2 \times 1$ **k**-points Monkhorst–Pack sets [24] within the bulk and surface Brillouin zones, respectively. Throughout the calculations we use the calculated GaAs equilibrium lattice constant of 5.57 Å.

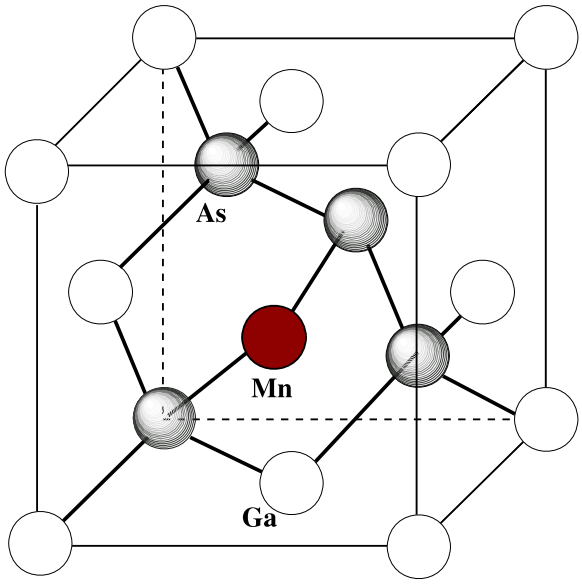

Figure 1. Crystal structure of the bulk GaAs with the Mn impurity being substituted at the Ga site.

To study the substitution of a single Mn atom at a Ga site we considered a large cubic unit cell of side 11.14 Å (containing 64 atoms). The Mn atom was held fixed and all other atoms were relaxed using total energy and atomic force minimization procedures. For surface calculations, we adopted a supercell approach. The surface unit cell was made up of nine $(1 \times 1)(110)$ atomic layers of GaAs and a vacuum region equivalent to six atomic layers. Mn substitution at a Ga site was considered in each of the top four layers of the slab. For both the clean GaAs(110) surface and the (Mn, Ga)–GaAs(110) surface, we kept the fifth layer (i.e. the middle layer) of the slab fixed and relaxed all other atoms.

For all σGGA + U calculations reported here, the value of the Hubbard correlation (U) was chosen to be 4.0 eV. This value is close to the choice $U = 3.5$ eV which was found to provide a good description of resonant photoemission results for $Ga_{1-x}Mn_xAs$ [25]. Many other researchers [17, 26–28] have also used a value close to 4 eV in their own calculations.

3. Results and discussion

3.1. Bulk calculations

3.1.1. Structural and magnetic properties. The optimized (relaxed) structure, schematically shown in figure 1, indicates that the nearest-neighbour As atoms have moved closer to the Mn atom. The calculated σGGA (σGGA + U) As–Mn bond length of 2.26 Å (2.32 Å) is smaller than the bulk GaAs bond length of 2.41 Å. The next-nearest-neighbour Ga atoms are at a distance of 3.91 Å (3.93 Å) from the Mn atom, as obtained from σGGA (σGGA + U) calculations. This calculated length is quite close to that for the bulk GaAs of 3.94 Å.

It should be mentioned that the electronic configuration of Mn in (Ga, Mn)As DMS is rather controversial [29].

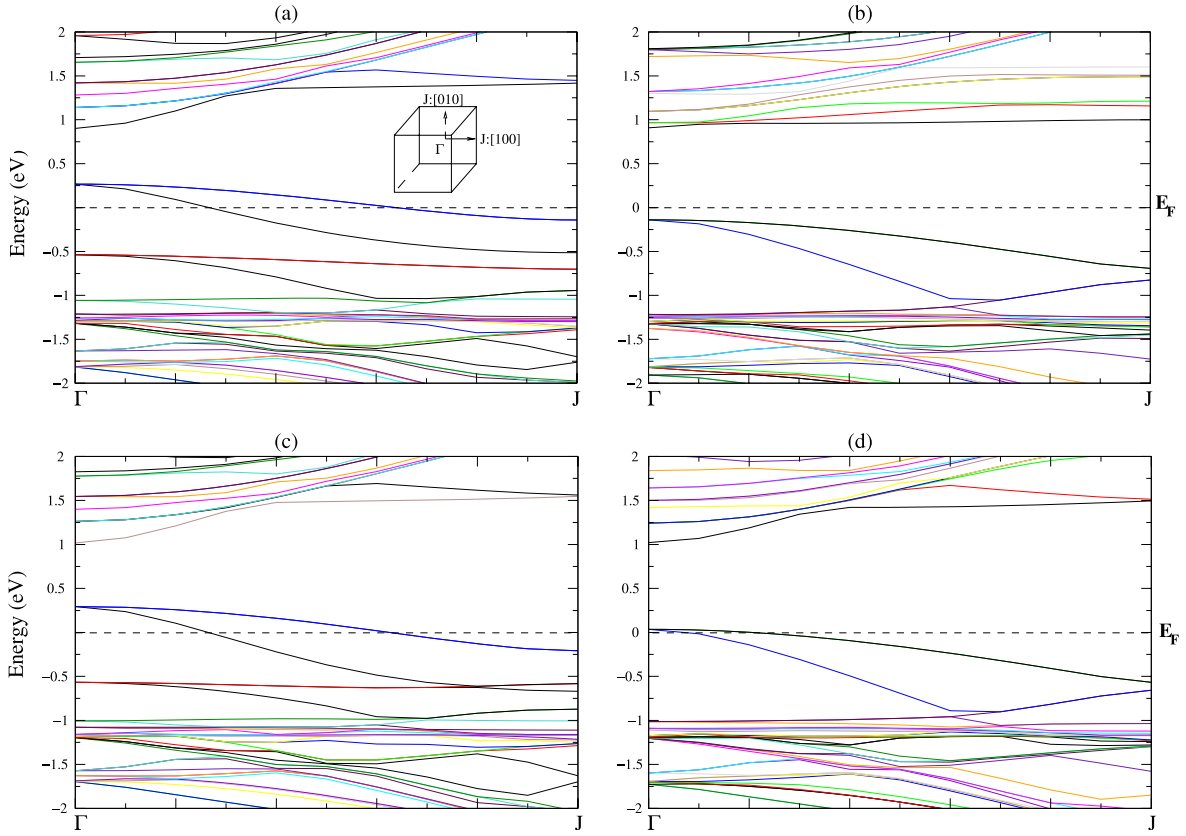

Figure 2. Electronic band structure for the (a), (c) majority and (b), (d) minority spin channels of the Mn impurity in the bulk GaAs within (top) σGGA and (bottom) σGGA + U. Also indicated are the bulk Brillouin zone for the periodic structure with a 64-atom cubic cell and the symmetry direction for the band structure plot.

Electronic and spin-flip Raman scattering experiments have revealed that the Mn impurity in (Ga, Mn)As can manifest itself in three different electronic configurations [30], with neutral Mn in the $3d^4$ configuration. Furthermore, Sapega *et al* [30] believe that the $3d^4$ configuration is relevant for the origin of ferromagnetism in (Ga, Mn)As DMS. Our calculations reveal that the local magnetic moment at the Mn site from the σGGA + U calculation is slightly larger (4.19 μ_B/Mn) than that from the σGGA (3.95 μ_B/Mn). These values are in good agreement with the values obtained from a previous theoretical work (3.80 μ_B/Mn and 4.20 μ_B/Mn using LSDA and LSDA+U with $U = 4.0$ eV, respectively) [31], but smaller than the SIC-LSDA value of 4.5 μ/Mn [7] as well as from experimental work (4.40 μ_B/Mn) [32]. Since the Mn magnetic moment is mostly derived from the polarization of the Mn d states, following Hund's rule our results suggest that the magnetic configuration of the Mn impurity can be described as $3d^4$ rather than $3d^5$. However, for a fuller understanding of the $3d^4$ configuration an examination of the Mn d orbitals and band structure of the Mn:GaAs system is required. This will be discussed in section 3.1.2.

3.1.2. Electronic properties. The σGGA and σGGA + U electronic band structures for both the majority and minority spin channels of the (Ga, Mn)As in the vicinity of the fundamental bandgap region are depicted in figure 2. Panels (a) and (b) of figure 2 show the majority and minority channels, respectively, in the absence of the Hubbard correction. Turning our attention to the majority spin channel (figure 2(a)), we clearly identify a doubly degenerate Mn 3d unoccupied state, approximately 0.25 eV above the Fermi level at the Γ point. The degeneracy of this band is removed for wavevectors away from the zone centre. The upper and lower sub-bands cut through the Fermi level, respectively, at approximately 65% and 25% along Γ–J in the Brillouin zone corresponding to the 64-atom cubic cell. Thus the system is metallic for the majority channel. The energetic position and dispersion of these bands clearly indicate the concept of a d-hole band. The minority channel, on the other hand, produces a semiconducting character with a GGA bandgap of 1.10 eV, which is smaller than the bulk GaAs bandgap (1.40 eV). Hence, the GaMnAs system is half-metallic. Our determination of the Mn acceptor level at 0.25 eV above the Fermi level is in agreement with the recent theoretical works by Wierzbowska *et al* [29] and Schulthess *et al* [7].

The σGGA + U calculations reveal a significant change in the width and dispersion of the spin-up Mn 3d states as shown in figure 2(c). The dispersion of both sub-bands has increased. Also, the splitting between the two sub-bands has increased, and the upper (lower) band crosses the Fermi level at a larger (shorter) distance along the Γ–J direction. Similar changes are observed for the minority (spin-down) states, with both sub-bands now almost touching the Fermi level near the Γ-point. This means that the system can be described as semi-

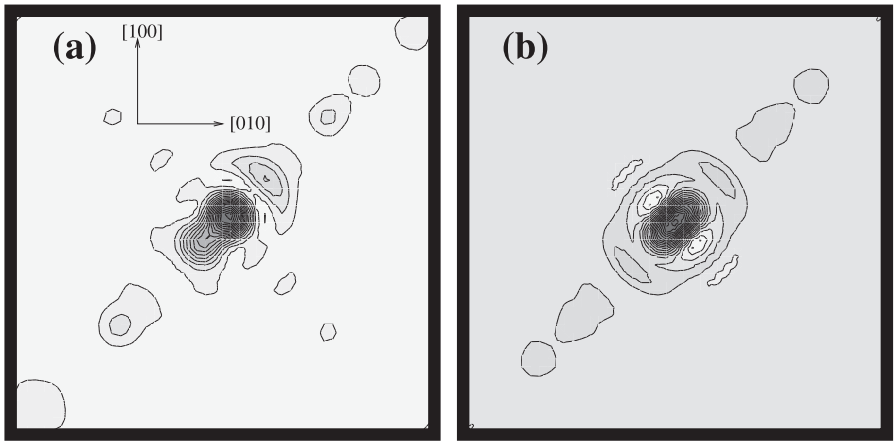

Figure 3. Partial charge density plots for (a) the degenerate band at the zone centre (i.e. Γ-point) just above the Fermi energy and (b) the higher of the two degenerate bands (which is the highest occupied band) at the zone edge (i.e. J point) of the Mn-doped GaAs structure within the σGGA framework. The Brillouin zone symmetry points Γ and J for the periodic structure with a 64-atom cubic cell are shown in figure 2.

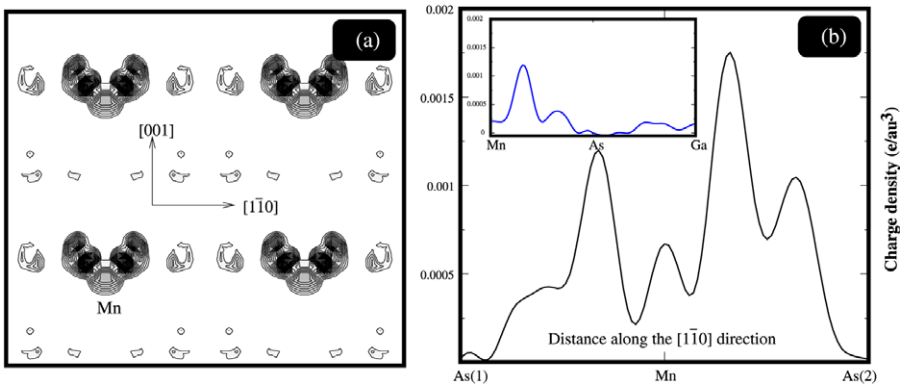

Figure 4. (a) The spatial structure of the Mn acceptor state, at 0.25 eV above the Fermi level, plotted on the [1$\bar{1}$0]-[001] plane. (b) Partial charge density of the acceptor state along the line joining the Mn atom with its nearest-neighbour As atoms. The inset represents the charge density of the acceptor state along the line joining the Mn atom with its nearest-neighbour As and Ga atoms. These plots are performed within the σGGA framework.

metallic rather than half-metallic. It is thus clearly seen that the Coulomb potential U plays an important role in the interaction of Mn d states with GaAs host valence bands. Our observations support the view expressed in the recent literature [7] that use of the standard band structure tools (for example, LSDA) is not enough to adequately describe the electronic structure of DMS.

The orbital nature of the electronic state close to the Fermi energy has been examined by plotting its partial charge density. Panel (a) in figure 3 presents the partial charge density plot for the (degenerate) band at the zone centre just above the Fermi energy and panel (b) shows the partial density for the higher of the two degenerate bands (which is the highest occupied band) at the zone edge J point. At the zone centre the degenerate band is contributed by the Mn d and As p orbitals, and at the zone edge the highest occupied band is contributed by the Mn d_{z^2} orbital. Together with the magnetic moment results, these observations suggest that the Mn impurity state should be described as $3d^4$ with a Mn-derived d-hole state above the Fermi energy.

Figure 4(a) shows the spatial structure of the Mn acceptor state at 0.25 eV above the Fermi level at the Γ-point. In this figure we have presented a contour plot in a plane passing thorough four Mn absorption sites and containing two Ga–As chains. In panel (b) we have presented line plots along As–Mn–As and Mn–As–Ga (inset). An inspection of the line plots reveals that this state has a strong covalent bonding contribution between Mn and its neighbouring As atoms. Also, it is clearly seen, both from the line plots and the contour plots, that the acceptor wavefunction is localized at the Mn site and spreads along the neighbouring As sites. There is a very low contribution along the Ga–As bonds. From these results we estimate the spread of the wavefunction not to be much larger than 2.6 Å around the substitutional site. Our findings for the anisotropic shape and extent of the wavefunction localization are similar to those obtained from the tight-binding calculations by Tang *et al* [33].

From the plots of the total density of states (DOS) in figure 5(a) we notice that the incorporation of Mn produces the following changes: there develops a peak and a shoulder in the region 0.0–0.7 eV below E_F, a redistribution of peaks in the range 3–4 eV below E_F and a redistribution of peaks in the region 3–4 above E_F. These observations, however, are in

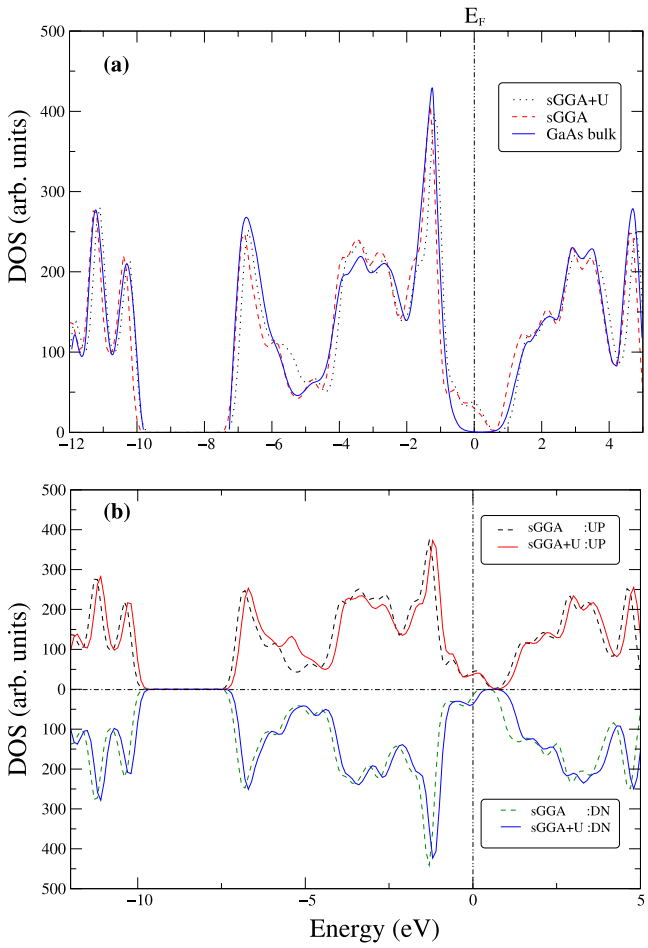

Figure 5. (a) The total density of state (DOS) for the 64-atom GaAs cubic cell with one Ga atom replaced by an Mn atom. (b) The spin-resolved density of states of the same structure. The spin-up/spin-down density of states is displayed above/below the abscissa axis.

agreement with previous reported results [7, 31]. Figure 5(b) shows the calculated spin-resolved total density of states using both the σGGA and σGGA + U approaches. It is clear that some peaks in both the majority and minority states are appreciably shifted from their original positions when the Coulomb correlation has been included. For the spin-up channel, Mn d peaks within the σGGA + U approach are observed at around 3.4 and 5.4 eV below the Fermi edge. The calculated peak at 3.4 eV is in excellent agreement with the peak at 3.4 eV observed in the photoemission spectrum data obtained by Asklund *et al* [34]. The calculated peak at 5.4 eV may be compared with the peak at 4.4 eV observed in the photoemission spectrum by Okabayashi *et al* [35]. The difference between the presently determined peak at 5.4 eV and the experimentally observed peak at 4.4 eV is likely to have several sources. The two most likely factors are experiments performed with a much lower Mn concentration and the use of a thin $Ga_{1-x}Mn_xAs$ film grown on GaAs(001) substrates. We also find a clearly noticeable empty peak at around 3.0 eV in the minority spin channel.

In figure 6 we have plotted the local density of states (LDOS) on the (001) plane by integrating density of states over an energy interval from E_F to E_F + 0.8 eV. Panels (a) and (b) show results from the σGGA + U and σGGA schemes, respectively. Within both approaches, we clearly observe the anisotropic 'butterfly shape' of the Mn d wavefunction [12]. It is also clear that the inclusion of the potential U changes the localization of the Mn wavefunction. This observation is in agreement with the results obtained by Kitchen *et al* [13] using experimental STM images of the (110) plane and theoretical LDOS plot on the (001) plane.

3.2. Surface calculations

3.2.1. Structural and magnetic properties. For the surface calculations we have initially considered two different configurations for adsorption of Mn atoms along the GaAs(110) surface trench: interstitial and substitutional. Since there is one more Ga atom for the structure with the Mn atom in the interstitial site than that for the structure with the Mn atom substituting for Ga, we must consider the chemical potential argument to compare the total energies of the two structures. Using the equation

$$\Delta E = E_{\text{inter}} - E_{\text{subst}} - \mu_{\text{Ga}}, \tag{1}$$

where E_{inter} and E_{subst} are the total energies of interstitial and substitutional site structures, respectively, and μ_{Ga} is the chemical potential of the Ga atom, we find that the substitutional site is the most energetically favourable by an energy of 0.15 eV/(1 × 1). We note that the preferable adsorption site of Mn on the GaAs(110) surface is in contrast to that found for the Si(001) surface where interstitial adsorption is favourable [36]. Having established the preferable adsorption site, we have also examined the most preferable atomic layer for the Mn atom to be substituted. Among various adsorption positions, as shown in figure 7, it is found that the Mn atom is most likely to replace the second-layer Ga atom. Our total energy calculations suggest that, compared to Mn adsorption in the second layer, adsorption in the first, third and fourth layers leads to a total energy increase by 0.1, 0.1 and 0.06 eV, respectively.

Our calculations suggest that the clean GaAs(110) relaxed structure is semiconducting with an energy gap of 0.72 eV and has a surface buckling of about 0.74 Å, resulting in a tilt of the chain of surface atoms by 29.30°. The buckling of the second layer is −0.13 Å, with Ga positioned higher than As. These findings are in good agreement with previously reported experimental and theoretical results [37–39]. Upon the adsorption of an Mn atom at the top layer the amount of surface tilt is found to be reduced to about 0.47 Å. However, the buckling of the second layer remains unchanged at −0.09 Å. These changes can be related to the smaller covalent radius of the Mn atom compared with Ga. The average bond length between the Mn atom and the nearest-neighbour As atoms is about 2.48 Å, which is slightly larger than the value in the bulk impurity situation. The surface GaAs bond length of 2.47 Å is found to be 2% larger than the calculated bulk bond length. The next-nearest-neighbour Ga atom is at a distance of 4.13 Å from the Mn atom. The strain resulting from such increases in interatomic distances is linked

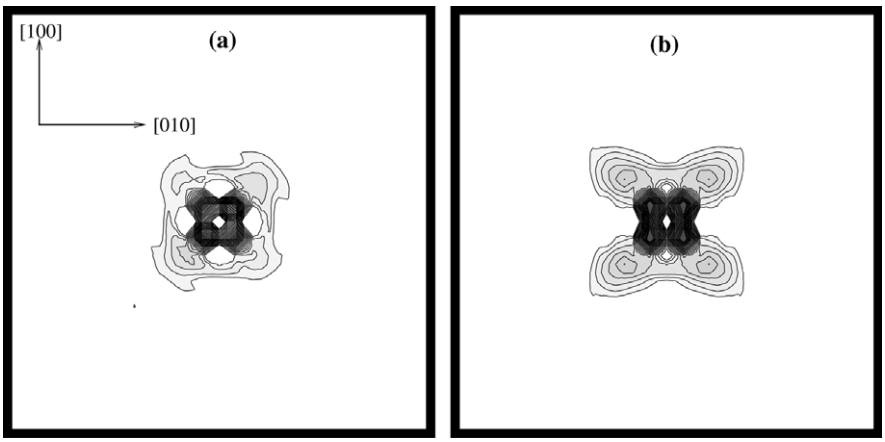

Figure 6. LDOS images for the empty states for the Mn impurity in bulk GaAs plotted on the (001) plane of the size of the GaAs cubic lattice constant: (a) with and (b) without U. The darker contours represent the maximum charge density. A voltage bias of $+0.8$ eV above the Fermi energy is applied.

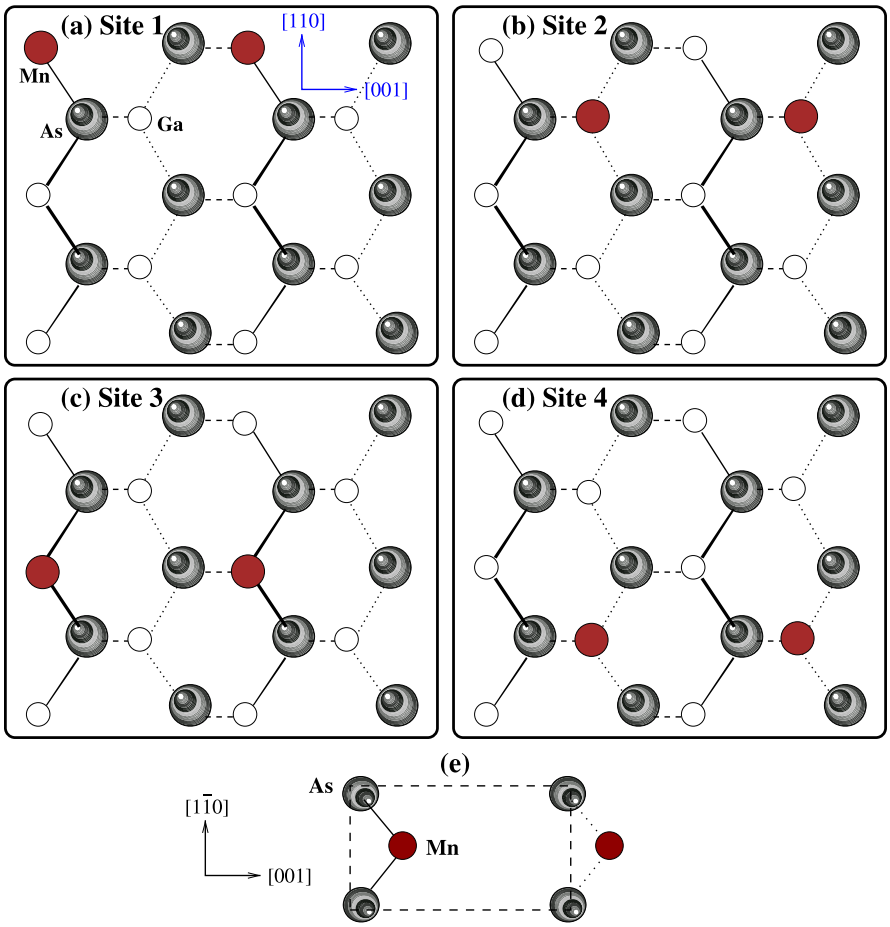

Figure 7. (a)–(d) Schematic side view of initial configurations for the adsorption of Mn in four different atomic layers on the GaAs(110)(1 × 1) surface. (e) Schematic top view of the surface unit cell.

to the significant reduction of the buckling in the top layer upon Mn adsorption. Slight changes in these lengths are observed when the Hubbard correction is considered in the calculation but not as much as in the bulk situation.

With Mn substitution at the Ga site in the second layer, the buckling of the top layer (0.84 Å) becomes larger than that on the clean surface, and the tilt in the second layer becomes -0.22 Å (the minus sign indicating that Mn is positioned higher than As). Clearly, these relaxation parameters are significantly different from both the clean surface and the surface with Mn adsorbed on the top layer. These relaxation parameters can be verified from intensity analysis of the low energy electron diffraction (LEED) pattern, ion-channelling analysis and angle-resolved photoemission

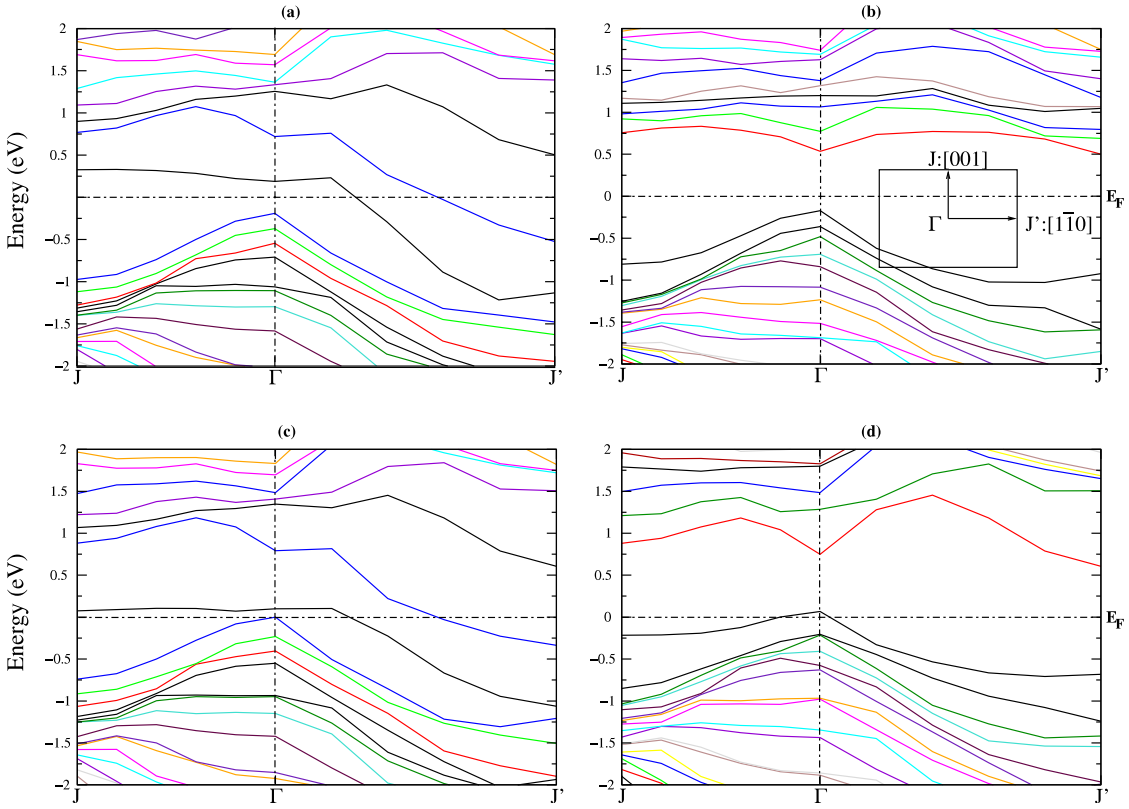

Figure 8. Surface electronic band structure for the (a), (c) majority and (b), (d) minority spin channels of the Mn/GaAs(110)(1 × 1) surface within (top) σGGA and (bottom) σGGA + U. The surface Brillouin zone is indicated.

spectroscopy (ARPES) studies, as these techniques have successfully been employed in the past to study III–V(110) surfaces (see, e.g., Duke [40]).

For Mn adsorption in the third and fourth layers, the buckling in the top layer reaches the clean surface value and the buckling of the Mn layer reduces to 0.03 Å and −0.08 Å, respectively. It is interesting to point out that the reduction in the magnitude and the sign variation in the Mn layer buckling with values of 0.46, −0.22, 0.03 and −0.078 Å in the first, second, third and fourth layers are similar to those found for the clean GaAs(110) surface (as found in this work and presented previously [38]).

Looking at the magnetic properties, our total energy calculations suggest that the system is ferromagnetic. The local magnetic moment of the Mn/GaAs(110) structure is calculated to be 4.12 μ_B/Mn, which is slightly smaller than the value obtained for the bulk impurity. This value increases to 4.32 μ_B/Mn when the Hubbard potential is included. This increase in the magnetic moment, due to U, agrees well with the previous study by Stroppa *et al* [39].

3.2.2. Electronic properties. Figure 8 shows the surface electronic band structures of the Mn/GaAs(110) surface, with and without the Hubbard potential U, in the vicinity of the fundamental bandgap region. For the σGGA calculations, we have identified two main surface states inside the GaAs bulk gap region. The majority channel shows that the system is metallic, with these states being fully unoccupied along the direction JΓ and fully occupied along the ΓJ′, as shown in figure 8(a) (the surface Brillouin zone is shown in the figure inset). The minority channel, figure 8(b), on the other hand, indicates that the system is semiconducting in nature. Having included the Hubbard potential in the band structure calculations, we clearly observe appreciable changes in both spin-up and spin-down channels. In the spin-up channel (figure 8(c)), we find that the lowest unoccupied surface state is pushed down towards the Fermi level by approximately 0.2 eV compared to the same state without including the Hubbard correction. The energy of the second-lowest unoccupied state is found to be increased by approximately 0.12 eV with respect to the same state if the Hubbard potential is not considered. However, the system remains metallic in this channel. The spin-down channel, on the other hand, produces a noticeable difference as shown in figure 8(d). Compared with the same channel in the absence of the Hubbard potential (namely figure 8(b)), we clearly notice that the highest occupied state is pushed up by approximately 0.52 eV and crosses the Fermi level. This actually leads to the metallicity of the system. These results again support the view held in the literature that the Hubbard potential plays an important role in determining the electronic properties of the DMS [7].

In order to gain information regarding changes in the wavefunction at and around the Mn adsorption site we have plotted the LDOS by considering the energy range E_F and E_F + 1.6 eV. The plots on the (1$\bar{1}$0) plane passing through the four different adsorption sites in figure 7 are depicted in

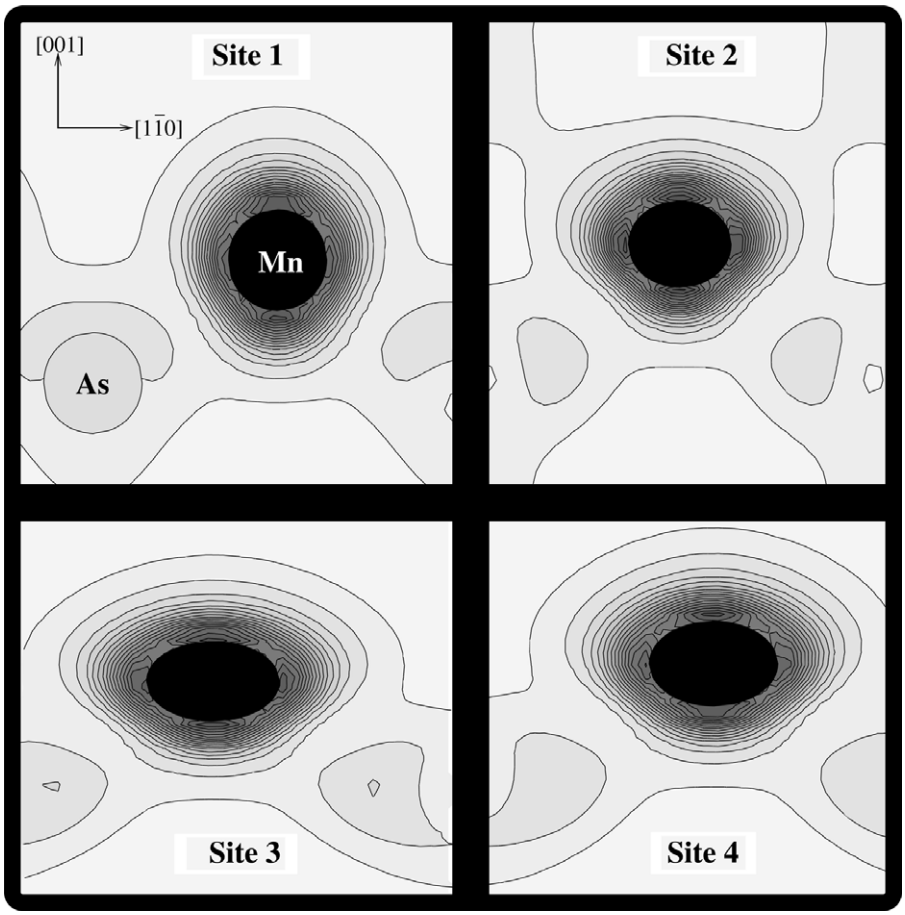

Figure 9. LDOS images for the empty states of the Mn/GaAs(110)(1 × 1) surface, in the σGGA framework, as a function of the adsorption sites shown in figure 7. The plot plane ([1$\bar{1}$0]–[001]) passes just over the Mn atom (and thus over the As atom) on the relaxed surface. For clarity only a small area around the Mn site is shown. The darker contours represent the maximum charge density. A bias voltage of 1.6 eV above the Fermi energy is applied.

figure 9. We clearly find that the localization and distribution of both the Mn and As wavefunctions differ as Mn resides deeper in subsurface layers. In particular, the deeper the Mn there is more spread in its wavefunction along the [001] direction.

We further examine our simulated STM image in the constant-height mode using the Tersoff–Hamann scheme [41]. In this scheme the tunnelling current is derived from the local density of states close to the Fermi energy E_F, i.e. an integrated local density of states from E_F to $E_F + V_B$, where V_B is the bias voltage. In our simulation we considered 1.6 eV for the bias voltage V_B. All the images shown in figure 10 are plotted at the horizontal plane 0.7 Å above the As atom on the clean relaxed surface. The image in panel (a) for the clean GaAs(110) surface shows, consistent with several previous works, the zig-zag pattern of the atomic sites on the top layer, with the Ga sites being much brighter than the As sites. Panels (b)–(e) show the image with Mn substituting Ga on the top, second, third and fourth atomic layers, respectively, on the area identical to that in panel (a). In general, the intensity and shape of the brightness change as Mn substitutes Ga in different layers. (The maximum intensities of the images are quoted in the figure caption.) When Mn substitutes Ga in the top layer (panel (b)), both anion (As) and cation (Mn) sites become almost equally bright. While the shape remains similar, the intensity of the protrusion at the cation site becomes larger than that for the clean surface. With Mn substituting Ga in the second layer (panel (c)) the anionic (cationic) sites becomes brighter (dimmer) and the shape of the maximum intensity elongates along [001]. There is a gradual change towards the clean surface as Mn substitutes Ga deeper into the third and fourth layers (panels (d) and (e)). For Mn substitution in the fourth layer, the shape and intensity of the image become similar to that for the clean surface.

We remark that in our models the Mn coverage of the surface is 0.5 monolayers. Yakunin *et al* [12] analysed samples where the concentration of the Mn substitutional impurity is extremely low (3×10^{18} cm^{-3}). Computational demand means that, using the fully *ab initio* scheme adopted in our work, we cannot analyse such a dilute regime and directly compare simulated and experimental STM images. This also means that we are not able to conclusively comment on the extent and influence of surface–tip interaction on the experimental data, or directly compare with the tight-binding STM simulations which were used by Yakunin *et al* [12]. We note, however, that the experimental images show large and small round features corresponding to As- and Ga-related surface states,

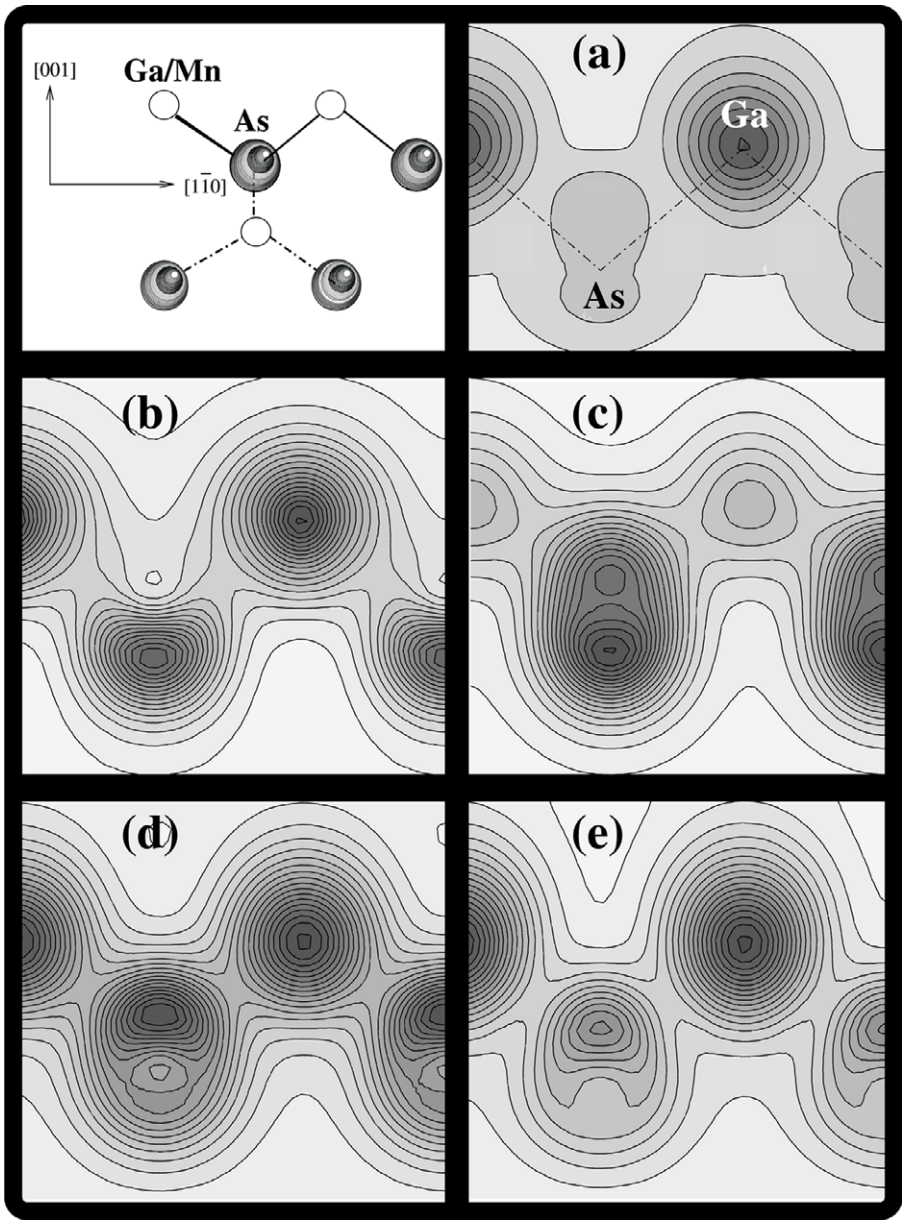

Figure 10. Simulated STM images, within σGGA, for the empty states, with a bias voltage of 1.6 eV, in the constant-height mode for (a) clean GaAs(110) surface and (b)–(e) Mn substituting Ga on the top, second, third and fourth atomic layers of the Mn/GaAs(110)(1 × 1) surface, respectively. The area of each image is $\sqrt{2}a \times 0.375\sqrt{2}a$, where a is the GaAs cubic lattice constant. The darker contours represent the maximum charge density. The image contours are equidistant with the maximum intensity of 0.014, 0.027, 0.014, 0.008 and 0.014 e au^{-3} for panels (a), (b), (c), (d) and (e), respectively. A schematic illustration of the zig-zag atomic chains in the slab is shown in the top left corner.

respectively. Such trends are replicated in our simulations and hence are supportive of the methodology employed to obtain our theoretical images. Furthermore, our theoretical results presented in figure 6 clearly show an anisotropic LDOS for an Mn impurity in bulk GaAs, which exhibits a resemblance to the experimentally observed wavefunctions in the STM images.

4. Summary and conclusion

From *ab initio* calculations, using the plane wave pseudopotential method and the density functional scheme, we have investigated the structural, magnetic and electronic properties of the (Ga, Mn)As dilute magnetic semiconductor (DMS) for both the bulk GaAs and GaAs(110) surface. With the Hubbard parameter $U = 4.0$ eV, the σGGA and σGGA + U calculations are properly compared. We find that the parameter U plays an important role in the determination of Mn d states and their interaction with the semiconducting host valence bands. Our calculations, using both the σGGA and σGGA + U, suggest that the Mn impurity in bulk GaAs can be described within the $3d^4$ scenario, with the energy level of the zone centre d state lying 0.25 eV above the Fermi level. Our simulated STM images for Mn/GaAs(110) indicate round protrusions at As sites and Ga sites, the latter being dependent on the Mn adsorption site (i.e. in different atomic layers). These results are supportive of

the experimental STM images obtained by Yakunin *et al* for the (Mn, Ga)/GaAs system with a very low Mn concentration.

Acknowledgments

A AlZahrani gratefully acknowledges financial support from King Abdulaziz University (KAU), Saudi Arabia. The calculations reported here were performed using the University of Exeter's SGI Altix ICE 8200 supercomputer.

References

[1] Ohno H 1998 *Science* **281** 951
[2] Ohno Y, Young D K, Beschoten B, Matsukura F, Ohno H and Awschalom D D 1999 *Nature* **402** 790
[3] Malajovich I, Berry J J, Samarth N and Awschalom D D 2001 *Nature* **411** 770
[4] Ku K C, Potashnik S J, Wang R F, Chun S H, Schiffer P, Samarth N, Seong M J, Mascarenhas A, Johnston-Halperin E, Myers R C, Gossard A C and Awschalom D D 2003 *Appl. Phys. Lett.* **82** 2302
[5] Chiba D, Takamura K, Matsukura F and Ohno H 2003 *Appl. Phys. Lett.* **82** 3020
[6] Linnarsson M, Janzén E, Monemar B, Kleverman M and Thilderkvist A 1997 *Phys. Rev.* B **55** 6938
[7] Schulthess T C, Temmerman W M, Szotek Z, Svane A and Petit L 2007 *J. Phys.: Condens. Matter* **19** 165207
[8] Grandidier B, Nys J, Delerue C, Stievenard D, Higo Y and Tanaka M 2000 *Appl. Phys. Lett.* **77** 4001
[9] Tsuruoka T, Tachikawa N, Ushioda S, Matsukura F, Takamura K and Ohno H 2002 *Appl. Phys. Lett.* **81** 2800
[10] Mahieu G, Condette P, Grandidier B, Nys J, Allan G, Stievenard D, Ebert P, Shimizu H and Tanaka M 2003 *Appl. Phys. Lett.* **82** 712
[11] Sullivan J M, Boishin G I, Whitman L J, Hanbicki A T, Jonker B T and Erwin S C 2003 *Phys. Rev.* B **68** 235324
[12] Yakunin A M, Silov A Yu, Koenraad P M, Wolter J H, Van Roy W, De Boeck J, Tang J-M and Flatté M E 2004 *Phys. Rev. Lett.* **92** 216806
[13] Kitchen D, Richardella A, Tang J-M, Flatté M E and Yazdani A 2006 *Nature* **442** 436
[14] Yakunin A M, Silov A Yu, Koenraad P M, Tang J-M, Flatté M E, Primus J-L, Van Roy W, De Boeck J, Monakhov A M, Romanov K S, Panaiotti I E and Averkiev N S 2007 *Nat. Mater.* **6** 512
[15] Jin X, Zhang M, Dong G S, Chen Y, Xu M, Zhu X G, Wang X, Lu E D, Pan H B, Xu P S, Zhang X Y and Fan C Y 1994 *Phys. Rev.* B **50** 9585
[16] Sandratskii L M, Bruno P and Kudrnovský J 2004 *Phys. Rev.* B **69** 195203
[17] Park J H, Kwon S K and Min B I 2000 *Physica* B **281/282** 703
[18] Fu H, Ye L, Zhang K and Xie X 1995 *Surf. Sci.* **341** 273
[19] Yang Z, Zhang K and Xie X 1997 *Surf. Sci.* **382** 100
[20] Hohenberg P and Kohn W 1964 *Phys. Rev.* **136** B864
[21] Perdew J P, Burke K and Ernzerhof M 1996 *Phys. Rev. Lett.* **77** 3865
[22] Vanderbilt D 1990 *Phys. Rev.* B **41** 7892
[23] Kohn W and Sham L 1965 *Phys. Rev.* **140** A1133
[24] Monkhorst H J and Pack J D 1976 *Phys. Rev.* B **13** 5188
[25] Okabayashi J, Kimura A, Rader O, Mizokawa T, Fujimori A, Hayashi T and Tanaka M 1998 *Phys. Rev.* B **58** R4211
[26] Shick A B, Kudrnovský J and Drchal V 2004 *Phys. Rev.* B **69** 125207
[27] Sanyal B, Bengone O and Mirbt S 2003 *Phys. Rev.* B **68** 205210
[28] Mahadevan P, Zunger A and Sarma D D 2004 *Phys. Rev. Lett.* **93** 177201
[29] Wierzbowska M, Sânchez-Portal D and Sanvito S 2004 *Phys. Rev.* B **70** 235209
[30] Sapega V F, Moreno M, Ramsteiner M, Däweritz L and Ploog K 2002 *Phys. Rev.* B **66** 075217
[31] Sato K, Dederichs P H and Katayama-Yoshida H 2006 *Physica* B **376/377** 639
[32] Ohno H 1999 *J. Magn. Soc. Japan* **23** 88
[33] Tang J-M and Flattè M E 2004 *Phys. Rev. Lett.* **92** 047201
[34] Åsklund H, Ilver L, Kanski J, Sadowski J and Mathieu R 2002 *Phys. Rev.* B **66** 115319
[35] Okabayashi J, Kimura A, Mizokawa T, Fujimori A, Hayashi T and Tanaka M 1999 *Phys. Rev.* B **59** R2486
[36] AlZahrani A Z, Srivastava G P and Miwa R H 2008 *Surf. Sci.* **602** 2789
[37] Duke C B 1983 *J. Vac. Sci. Technol.* **1** 732
[38] Srivastava G P 1992 *Phys. Rev.* B **46** 7300
[39] Stroppa A, Duan X and Peressi M 2006 *Mater. Sci. Eng.* B **126** 217
[40] Duke C B 1993 *J. Vac. Sci. Technol.* B **11** 1336
[41] Tersoff J and Hamann D R 1985 *Phys. Rev.* B **31** 805